

Optimal Control of Piezoceramic Actuators

Jinghua Zhong^a, Stefan Seelecke^b, Ralph C. Smith^c, Christof Bueskens^d

^{a,b}Mechanical and Aerospace Engineering, NC State University, Raleigh, NC, USA 27695

^cCenter for Research in Scientific Computation, NC State University, Raleigh, NC, USA 27695

^dDepartment of Applied Mathematics, University of Bayreuth, Bayreuth, Germany 95440

ABSTRACT

This paper presents the first results of an optimal control approach to piezoceramic actuators. A one-dimensional free energy model for piezoceramics recently proposed by Smith and Seelecke is briefly reviewed first. It is capable of predicting the hysteretic behavior along with the frequency-dependence present in these materials. The model is implemented into an optimal control package, and two exemplary cases are simulated to illustrate these features and the potential of the method.

Keywords: optimal control, hysteresis, free energy model, piezoceramic actuators

1. INTRODUCTION

Actuators from piezoceramic materials have established themselves in a large number of applications ranging from active vibration control to nano-scale positioning tasks. This is due to their high-frequency response behavior and their essentially infinite resolution. In particular, in the area of nano-scale positioning, e.g., scanning microscopy applications, optical fiber alignment, or general nano-manufacturing tasks, one is interested in combining these two attractive features. Even though tremendous progress has been made in the area of hardware development to enable higher speed in sensing and measuring, it appears that the control algorithms represent the bottleneck with respect to improved performance. Most controllers are based on conventional PID feedback methods, which have originally been developed for linear systems. Piezoceramics, however, can be considered to behave linearly only to about 15% of their maximum field strength. If one is to make more efficient use of the actuator, one has to account for the highly nonlinear and hysteretic material behavior and incorporate it into the control algorithm.

A first step in the direction of improved control algorithms is a method known as adaptive feedforward control. It is based on the representation of the system and the control as finite impulse response filters (FIR), the coefficients of which are determined by least mean square algorithms. A detailed overview of its application to the control of smart structures is given in [1], see [2] and [3] for a general theory of adaptive filters and design. The method, however, is restricted to linear systems or systems that can be linearized and thus is only applicable in the low drive level range. A next step is the introduction of non-linear models into the feedforward control. In [4], a feedforward model-reference control method has been applied to improve the scanning accuracy in a scanning tunneling microscope. Three different models have been used, however, all of them imply that the hysteresis non-linearity has either local memory or symmetrical behavior, both of which do not exactly represent the hysteretic behavior of piezoceramic actuators. Also, a pure feedforward method in a non-linear environment is always prone to drift away from the desired behavior, so a logical improvement is a hybrid method, which couples a non-linear model with a feedback controller. This method is also known as inverse compensator method, and it has been successfully applied to the control of piezoceramic actuators in [5] and [6], magnetostrictive transducers in [7], and shape memory alloys in [8], [9] and [10]. A general overview can be found in [11] and [12]. All these methods have in common that they try to address robustness and stability issues, but none of them takes optimality into account. Optimal control is attractive as it aims to minimize some cost functional like

^a Email: jzhong2@unity.ncsu.edu

^b Email: stefan_seelecke@ncsu.edu - corresponding author

^c Email: rsmith@eos.ncsu.edu

^d Email: Christof.Bueskens@uni-bayreuth.de

energy consumption or final time. Some attempts toward this end have been made for shape memory alloys and magnetostrictive materials. In [13], a SMA hysteresis model is implemented into an optimal control code to control the shape of an adaptive beam actuated by a SMA wire. In [14] and [15], the authors compute an optimal control for a magnetostrictive actuator based on an infinite time horizon optimal control problem. Due to the large computational effort, these approaches have up to only recently been confined to offline simulations. In [16], an approach for a magnetostrictive actuator is presented, which combines perturbation feedback control with a nonlinear optimal control method, thus allowing an online implementation. In a series of papers [17], [18], [19] and [20], a similar method has been developed for the optimal control of shape memory alloy actuators. It is based on the concept of a parametric optimal control process combined with a sensitivity analysis, and it reduces the computation time for an optimal control process to the order of nanoseconds. Thus, it has become clearly real-time capable, and, in particular through the combination with a strongly physics-oriented model for the material behavior, the method can be regarded as the basis for the development of extremely efficient control algorithms for active materials actuators.

Due to their close resemblance in microstructure and similarity in macroscopic behavior such as hysteresis, non-linearity and Curie temperature, SMAs, piezoceramics and magnetostrictive materials can be described in a unified way [21]. In [22], Smith and Seelecke proposed a free-energy-based model for homogeneous single crystal piezoceramics, which is a direct extension of the Müller-Achenbach-Seelecke theory for shape memory alloys [13,18]. The effects of non-uniform lattices, variations in effective fields, and polycrystallinity are introduced by incorporating appropriate distributions in the free energy formulations. The physical parameters in the model greatly alleviate the difficulty to accommodate changing operating conditions for traditional Preisach models, which typically use a large number of unphysical parameters (see [23] for details).

In this paper, we combine the above ideas to present an implementation of a piezoceramic actuator model into an optimal control code. The implementation does not address real-time aspects yet, but as a first step, focuses on the basic off-line control problem. We briefly review the model in section 2, and based on a preliminary implementation of the concept of distributions, we illustrate the model’s hysteretic properties and in particular its capability of reproducing the frequency-dependent behavior observed in these materials. In the final section, we discuss the implementation into an optimal control code and present two non-trivial control problems addressing the material properties mentioned above.

2. A MODEL FOR PIEZOCERAMIC MATERIALS

2.1 Single crystal

This section introduces the model, which is used in the subsequent optimal control problems. Numerous models have been proposed in the past decades to model hysteresis, most of which are motivated by research in magnetic materials. For piezoceramics, microscopic models at the grain or lattice level are rarely employed for control purposes due to the large number of parameters and states involved. Macroscopic models are typically low-order and based on empirical principles, e.g. the Preisach model [26] and its variations [27,28], but the absence of physical parameters makes it difficult to incorporate frequency, temperature or load dependencies and adapt to changing operating conditions. Also, most of these models only consider part of the hysteresis loop with a unipolar field [6], which limits the available stroke of the actuators. Semi-macroscopic (mesoscopic) models, including the model used in this paper, are derived from energy principles and try to combine microscopic mechanisms with macroscopic averages to obtain physical parameters [29,30]. They usually provide a good compromise between capturing the physical properties of the material and being computationally efficient, so that they represent a good choice for the implementation into a control algorithm.

In this paper, we use the one-dimensional energy model proposed by Smith and Seelecke for piezoceramics. It is developed with the assumption that dipoles in a single crystal with uniform lattice spacing have two orientations, which are denoted by (+) and (−), depending on whether the Ti^{4+} ion is displaced upward or downward with respect to the center of symmetry (see Figure 1).

For a typical mesoscopic domain consisting of a number of equally poled lattice cells, the model assumes the following multiparabolic representation for the Helmholtz free energy density ψ as a function of the polarization P :

$$\psi(P) = \begin{cases} \frac{1}{2} E_1 (P + P_T)^2 & , P \leq -P_1 \\ \frac{1}{2} E_1 (P - P_T)^2 & , P \geq P_1 \\ \frac{1}{2} E_1 (P_1 - P_T) \left[\frac{P^2}{P_1} - P_T \right] & , |P| < P_1 \end{cases} \quad (1)$$

In Eq. (1), P_T , P_1 and E_1 are related to physical properties, which can be extracted from an electric field vs. polarization diagram. P_T denotes the remnant polarization, P_1 the onset of the switching process, and E_1 is the reciprocal of the slope of the (E, P) curve (see the bottom row of Figure 2).

The switching processes in the material can be interpreted as phase transformations with the polarization as the order parameter. The kinetics of these phase transformations are determined by the electric-field-dependent barriers and minima in the Gibbs free energy, which is related to the Helmholtz free energy in Eq. (1) through the Legendre transformation $G = \psi - EP$. This dependence is illustrated in Figure 2 for increasing field values (from left to right) together with the corresponding polarization vs. electric-field behavior.

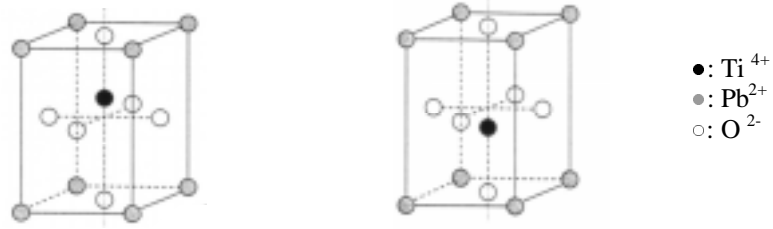


Figure 1 PbTiO_3 crystal lattice cells with positive and negative polarization

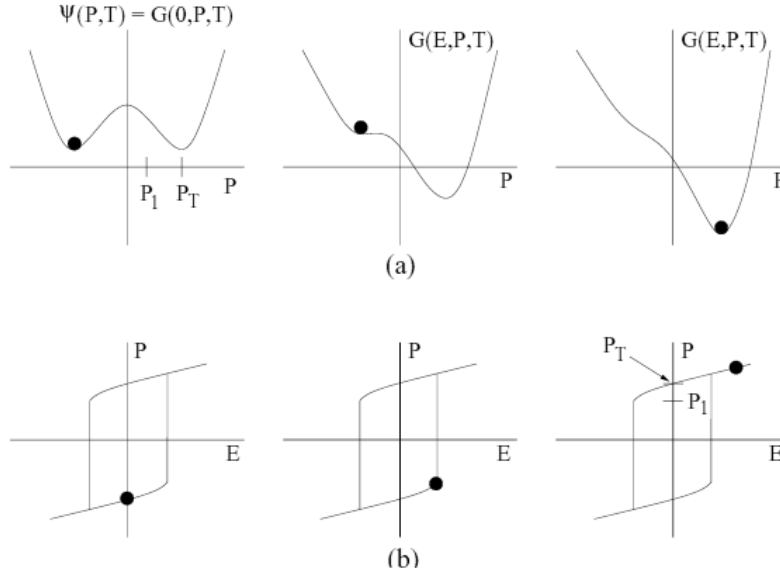


Figure 2 (a) Helmholtz energy ψ and Gibbs energy G for increasing field E ; (b) Polarization P as a function of E for a single crystal with uniform lattice.

Due to the ever-present thermal activation, all domains fluctuate about their equilibrium polarization values. From Boltzmann principles, the probability of attaining an energy level G is

$$\mu(G) = Ce^{-G/kT}, \quad (2)$$

where k denotes Boltzmann's constant. The expected average polarizations due to domains with positive and negative polarizations are then given by

$$\langle P_+ \rangle = \frac{\int_{P_1}^{\infty} P e^{-G(E,P,T)V_D/kT} dP}{\int_{P_1}^{\infty} e^{-G(E,P,T)V_D/kT} dP}, \text{ and} \quad (3)$$

$$\langle P_- \rangle = \frac{\int_{-\infty}^{-P_1} P e^{-G(E,P,T)V_D/kT} dP}{\int_{-\infty}^{-P_1} e^{-G(E,P,T)V_D/kT} dP}, \quad (4)$$

and the average polarization for the whole actuator is

$$\bar{P} = x_+ \langle P_+ \rangle + x_- \langle P_- \rangle, \quad (5)$$

where x_+ and x_- denote the fractions of domains with positive or negative polarization respectively. These phase fractions evolve in time according to the differential equations

$$\begin{aligned} \dot{x}_+ &= -p_{+-}x_+ + p_{-+}x_- \\ \dot{x}_- &= -p_{-+}x_- + p_{+-}x_+ \end{aligned} \quad (6)$$

which can be simplified to

$$\dot{x}_+ = -p_{+-}x_+ + p_{-+}(1 - x_+) \quad (7)$$

through the identity $x_+ + x_- = 1$. Here p_{+-} and p_{-+} denote the transition probabilities of a domain switching from one polarization to the other. They are computed by

$$\begin{aligned} p_{+-} &= \frac{1}{\tau_x} \frac{e^{-G(E,P_1(T),T)V_D/kT}}{\int_{P_1}^{\infty} e^{-G(E,P,T)V_D/kT} dP} \\ p_{-+} &= \frac{1}{\tau_x} \frac{e^{-G(E,-P_1(T),T)V_D/kT}}{\int_{-\infty}^{-P_1} e^{-G(E,P,T)V_D/kT} dP}, \end{aligned} \quad (8)$$

where τ_x is the relaxation time of the material and V_D denotes the activation volume of the domain. The ratio V_D/kT determines the fluctuation of polarization about the equilibrium values due to thermal activation, and together with τ_x , this ratio dictates the frequency dependence of the hysteresis loops. The solution of equation (5) specifies the hysteretic relation between E and P , as is depicted in Figure 2.

2.2 Polycrystalline materials

As the above model describes perfect single crystal behavior, realistic actuators are neither perfect nor are they single crystals. Rather they exhibit inhomogeneities due to lattice imperfections, impurities, grain boundaries, etc., which lead to variations in the energy barriers, depending on the location of the domain under consideration. Following again the ideas outlined in [22] and [24], we take these variations into account by introducing a distribution in the energy barriers.

In particular, we consider the lattice parameter $\tilde{E}_1 = E_1(P_T - P_1)$ to be normally distributed with mean \bar{E} . The total polarization is then given by

$$P(E) = \int_0^\infty \bar{P}(E, \tilde{E}_1) f(\tilde{E}_1) d\tilde{E}_1 \quad (9)$$

with the density

$$f(\tilde{E}_1) = Ce^{-(\tilde{E}_1 - \bar{E})^2/b} \quad (10)$$

Other aspects such as variations in the effective field can be addressed similarly by introducing additional distributions for the corresponding parameters [22]. To simplify the algorithm and reduce computational cost for the solution of the optimal control problem, only the distribution of energy barriers is considered and implemented in this paper.

2.3 Numerical implementation

In [18], the integral in Eq. (9) is numerically solved by a Gaussian quadrature method. A set of single crystal ODEs must be solved at each of the abscissae points, so that the number of Gauss points determines the size of the system. Obtaining a smooth hysteresis curve thus requires the solution of a large number of ODEs, which severely reduces the computational speed. In [24], the authors suggest an efficient scheme to calculate the overall polarization from the switching of individual domains by utilizing algebraic matrix operations, but it is valid only for the limiting case of zero thermal activation, and is not able to account for effects related to different loading rates. Within the context of time-dependent processes, we are particularly concerned with the model's capability of reproducing the frequency dependent response correctly. In order to retain this capability, we choose yet an alternative way to implement the distributions, which at the same time, proves to be highly computationally efficient.

To reduce computational cost, we implement the distribution into the ODE by parameterizing the process of the phase transition. Instead of calculating many domains simultaneously, we consider a representative domain, which is most likely to transform next at a given value of the phase fraction and the prescribed electric field. The lattice parameter \tilde{E}_1 for this domain is calculated from the current phase fraction and loading history. This way, only one ODE needs to be solved. A preliminary implementation of this concept, which is used for the optimal control code, correctly predicts the outer hysteresis loop, although further development is necessary to retain the correct inner loops. Details will be given in a forthcoming paper [32]. Figure 3 illustrates the model's capability of capturing the frequency dependence for two typical values. Note the dramatic impact on the shape of outer and inner hysteresis loops. The parameter values used for the simulations throughout the paper are: $T = 273.0$ K, $V_D = 1.0 \times 10^{-22}$ m³, $\tau_x = 1.0 \times 10^{-2}$ s⁻¹, $P_1 = 0.275$ C/m², $P_T = 0.26$ C/m², $E_1 = 6.67 \times 10^7$ V·m/C, $b = 2.0 \times 10^{12}$, and $\bar{E} = 1.0 \times 10^6$ V/m.

3. OPTIMAL CONTROL

3.1 Optimal control problem

In the following section, we will study the solution of the optimal control problems. For simplicity, we consider a one-dimensional piezoceramic stack actuator in the absence of mechanical loads, and, instead of tracking the displacement, we consider the polarization as the quantity that can be prescribed.

Thus we prescribe the set-point polarization $P_{set}(t)$, and solve for the electric field function $E(t)$, which minimizes the following cost functional

$$J = \int_0^T [P(t) - P_{set}(t)]^2 dt . \quad (11)$$

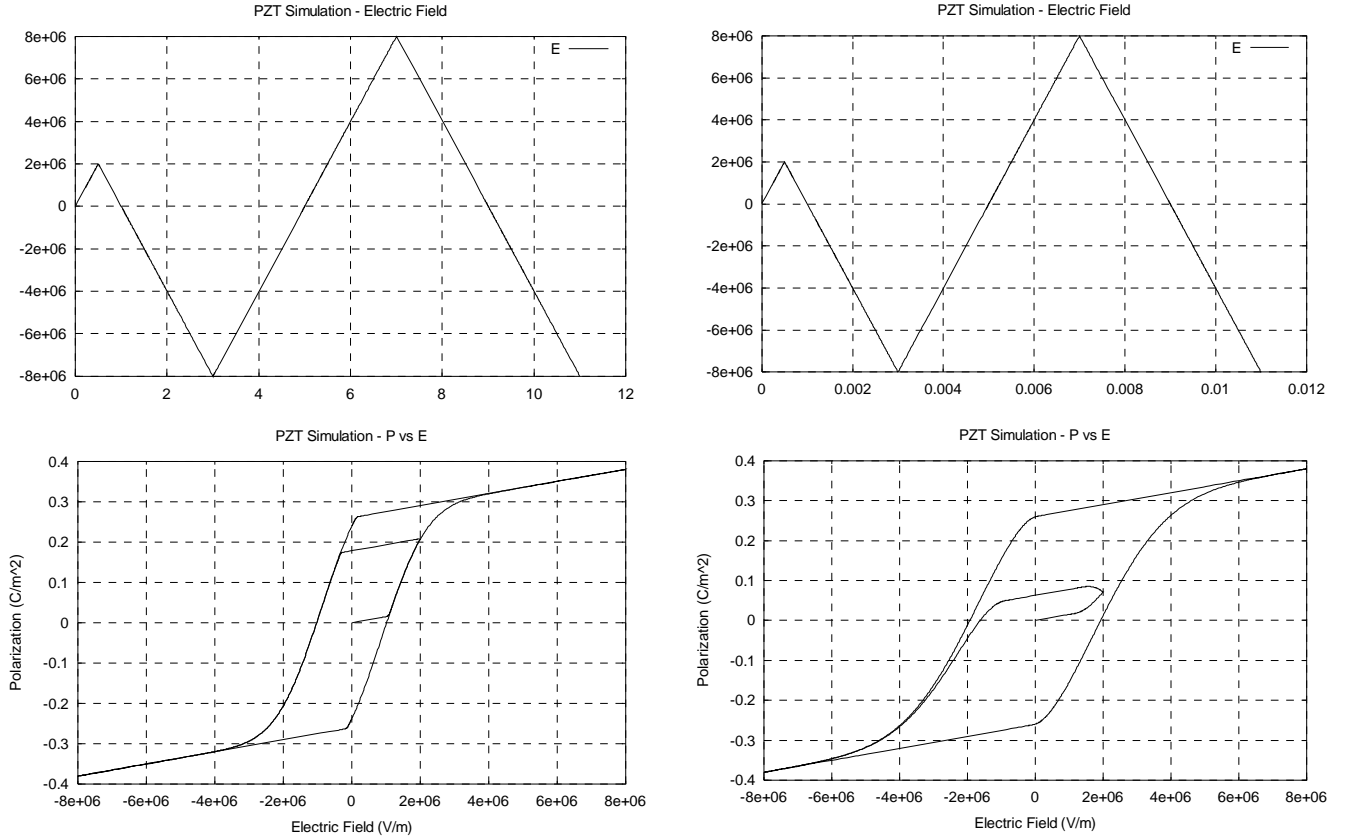


Figure 3 Left: hysteresis curve at 0.125Hz, Right: hysteresis curve at 125Hz

This ensures that the set point is reached in the shortest time possible and subsequently maintained. The minimization is subject to the following constraints

$$\begin{aligned} \dot{x} &= f(x(t), E(t)), \\ x(0) &= x_0, \quad \text{and} \\ |E(t)| &\leq E_{\max} . \end{aligned} \quad (12)$$

Equation (12)₁ represents the model equation, which describes the switching processes in the actuator, Eq. (12)₂ are the initial conditions of the process, and Eq. (12)₃ are box constraints for the control, representing the fact that only a finite electric field can be applied to the actuator.

For the numerical solution, we have implemented the model from the previous section into the optimal control package NUDOCSS developed by Büskens [25]. Based on a direct approach, NUDOCSS discretizes the control and transforms the original control problem into a nonlinear optimization problem. The control function (the electric field $E(t)$) can be either assumed piecewise linear or interpolated by higher order splines. We have used the piecewise linear option for simplicity and faster calculation.

The differential equations for the state variables are integrated by an implicit Runge-Kutta scheme (RADAU IIa) using the efficient and robust RADAU5 routine from the book of Hairer and Wanner [31]. NUDOCSS then solves the resulting NLP problem with a sequential quadratic programming method.

3.2 Case 1: Single-level set point

We start with a simple case, which allows illustrating the rate-dependent behavior of the actuator. From an initial polarization $P(0) = 0 \text{ C/m}^2$, the set point rises linearly to a new level $P_{set} = 0.2 \text{ C/m}^2$ at a rate of $500 \text{ C/m}^2/\text{sec}$ within 4 ms. The constraint E_{max} has been set to 6 MV/m.

The four plots in Figure 4 show the time evolutions of the phase fraction $x(t)$ and polarization $P(t)$ along with the value of the cost functional and the optimal electric field $E(t)$ (from upper left to lower right). Figure 5 shows the hysteretic behavior of the actuator in a P - E plot.

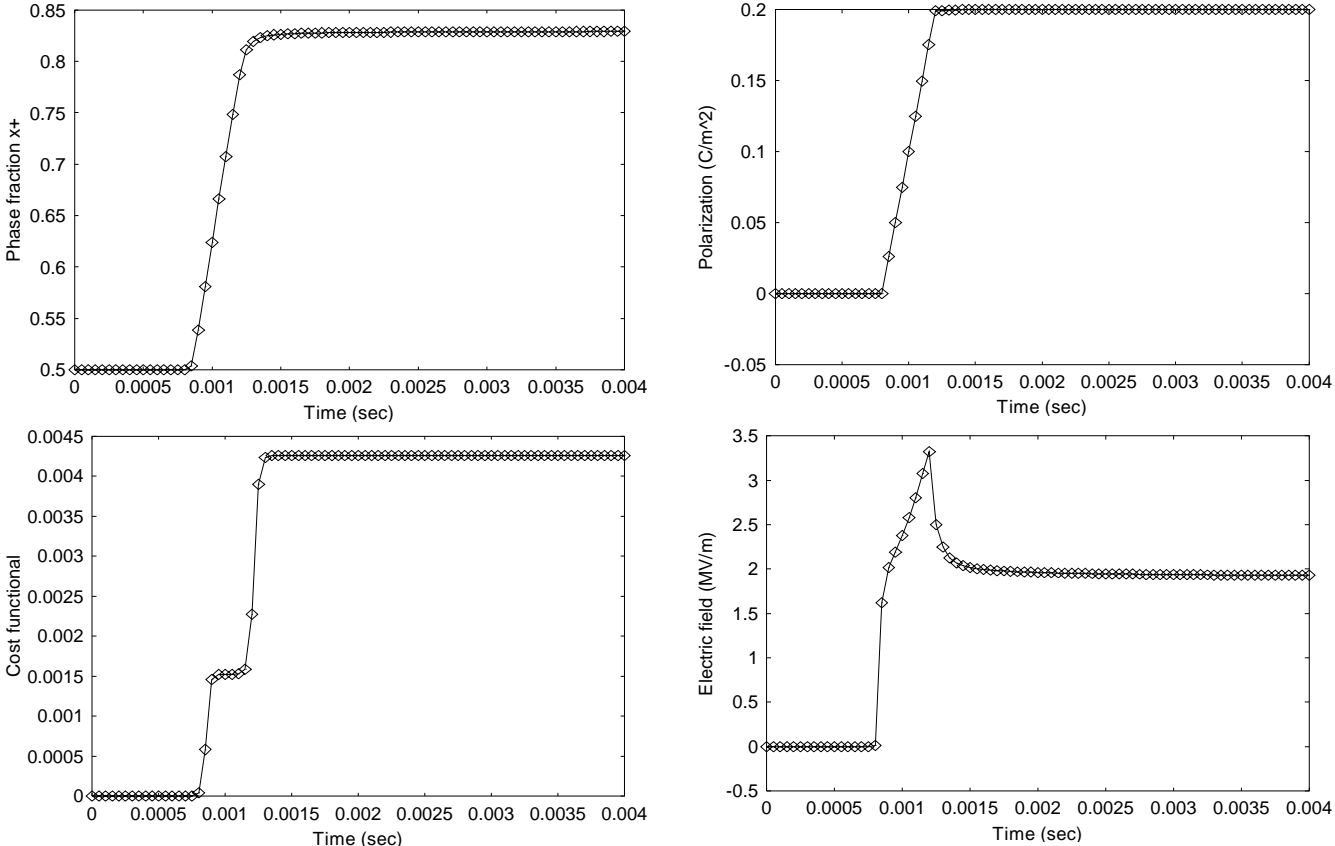


Figure 4 Optimal control of piezoceramic polarization (Case 1)

The polarization calculated from the optimal solution follows the set-point function closely, especially in the middle of the rising process, which can be seen from the cost functional increasing only very little during this phase of the process. Most of the error occurs near the beginning and the end of the transition. In the mean time, the phase fraction increases monotonously from 0.5 to 0.83. The electric field, however, exhibits some interesting features due to the nonlinear and hysteretic behavior of piezoceramics at different loading rates.

When a positive electric field is applied to the piezoceramic actuator, the increase in polarization contains two different terms. The first term is proportional to the applied field and time independent. The second term is governed by the evolution of the phase fraction and as such is time dependent. The model automatically accounts for this behavior through a suitable choice of relaxation time and activation volume, and consequently, the piezoceramic actuator exhibits different shapes of hysteresis at different loading frequencies.

As we can see from Figure 4, the electric field starts with a sharp increase, which is equivalent to a loading frequency of 1250 Hz, then continues to increase at a roughly 10 times slower rate, until it reaches the peak of 3.3 MV/m. At this electric field value, the polarization has almost reached the required set point, but the phase transition has not yet completed. Some domains of negative phase continue to change into positive phase, which will increase the overall polarization of the actuator. To compensate for this increase, the electric field then decreases asymptotically to about 1.9 MV/m. This process is better illustrated in Figure 5, which shows the optimal solution along with hysteresis loops at three different loading frequencies.

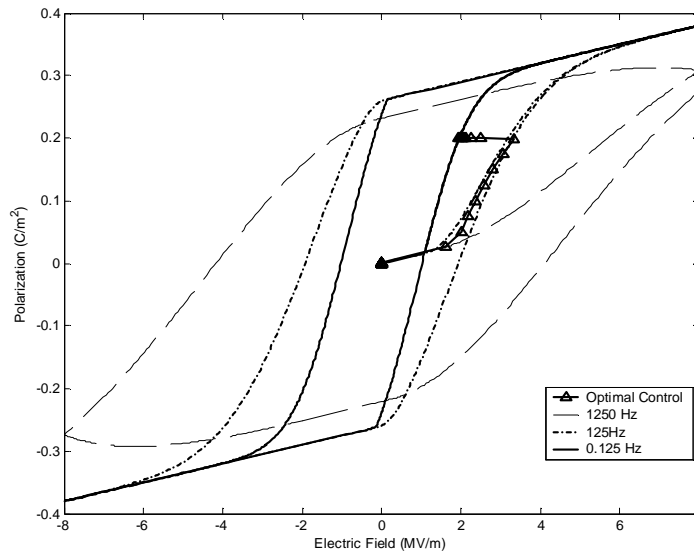


Figure 5 P-E behavior of the optimal solution (Case 1)

In Figure 5, the actuator first follows the hysteresis curve at the highest frequency (the widest loop), then as the rate of the electric field decreases, it overlaps with the curve at a lower loading frequency, and finally relaxes to a point on the quasistatic outer loop (0.125 Hz). At a frequency of 0.125 Hz, the effect from the relaxation time of the domains is negligible because the domains now have enough time to complete the phase transition as the field increases. If no optimal control is applied, the same polarization set point can be achieved by slowly increasing the electric field. The actuator would then follow the hysteresis curve of 0.125 Hz.

3.3 A more complex set-point function

Due to hysteresis, the same polarization may require a different electric field if the loading history is different. We proceed with the prescription of a more complex set-point function to verify the model’s ability to predict the polarity of the electric field needed for a positive polarization with different history. The set-point polarization first increases from

0.0 C/m² to 0.1 C/m² linearly at a rate of 500 C/m²/sec, holds for a period of time, increases again to 0.2 C/m² at the same rate, holds the value, and then decreases back to 0.1 C/m² at a rate of -500 C/m²/sec. In the simulation, the control process has a total duration of 4 ms, and is discretized using 81 points (NDISKRET=81 in NUDOCCCS). E_{\max} is set to 6 MV/m. The four plots in Figure 6 show the time evolutions of the phase fraction $x(t)$ and polarization $P(t)$ along with the value of the cost functional and the necessary electric field $E(t)$ (from upper left to lower right). Figure 7 shows the hysteretic behavior of the actuator in a P - E plot.

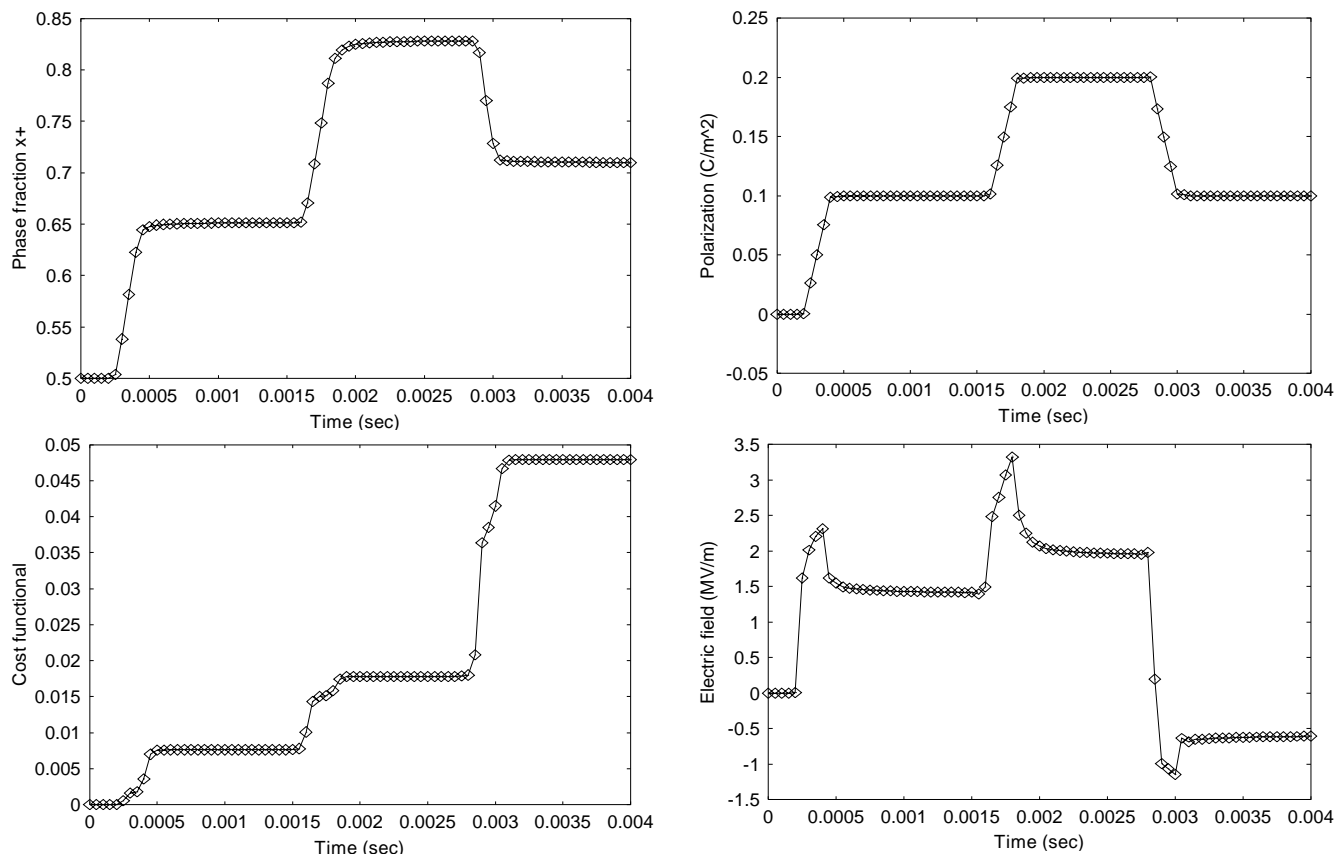


Figure 6 Optimal control of piezoceramic polarization (Case 2)

In this case, not surprisingly, the model predicts similar shapes of optimal electric fields for the actuator. The electric field increases first to a high value, and then drops back to a lower value as the piezoceramic material relaxes, forcing the polarization to follow the set point. The maximum electric field needed for the second set point of 0.2 C/m² is almost the same as that of the previous section, and the field also decreases at the same rate to the same final value to maintain the polarization. As Figure 7 shows, in following the three set points, the actuator first follows the hysteresis loop of a higher frequency but always comes back to a point on a loop of low frequency.

For the first and third set point, although they have the same polarization of 0.1 C/m², the model predicts completely different phase fractions and electric fields. Obviously, this is due to the difference in the history. For the first set point, a positive electric field is applied, because the initial positive phase fraction needs to be increased. To reach the third set point, the hysteresis has to be traversed, and a negative electric field has to be applied in order to reach the same polarization value as for the first set point.

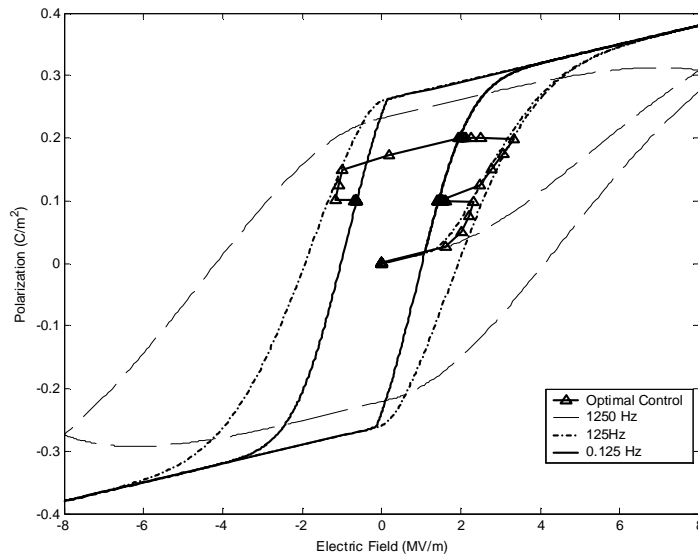


Figure 7 P-E behavior of the optimal solution (Case 2)

4. CONCLUSION

The paper introduced an implementation of an energy-based model for the simulation of polycrystalline piezoceramic materials. The model reproduces the outer hysteresis loops typically observed in these materials correctly, although further development is needed for a better simulation of minor loops. It was also shown, that the effect of varying loading rate is captured, and both these effects were illustrated to play an important role in typical control problems. The model has been implemented into an optimal control code, which does not only compensate for the non-linear and hysteretic material behavior, but allows optimality criteria like speed of adjustment to be taken into account. This first implementation demonstrated the feasibility of the concept by successfully computing offline solutions, while future work will focus on implementing real-time concepts recently developed by the authors for shape memory alloys [16,17].

ACKNOWLEDGEMENTS

The research of S.S and J.Z was supported in part through the NSF grant DMI-0134464. The research of R.C.S. was supported in part through the NSF grant CMS-0099764 and in part by the Air Force Office of Scientific Research under the grant AFOSR-F49620-01-1-0107.

REFERENCES

1. R. L. Clark, W. R. Saunders, and G. P. Gibbs, *Adaptive Structures: Dynamics and Control*. John Wiley, 1998.
2. S. M. Kuo and D. R. Morgan, *Active Noise Control Systems*. John Wiley and Sons, 1996.
3. B. Widrow and S. D. Stearns, *Adaptive Signal Processing*. Prentice Hall, Englewood Cliffs, NJ, 1985.
4. S. Jung and S. Kim, Improvement of Scanning Accuracy of PZT Piezoelectric Actuators by Feedforward Model-Reference Control, *Precision Engineering*, 16, pp. 49–55, 1994.
5. H. Janocha, *Adaptronics and Smart Structures*, chapter Actuators in Adaptronics, Springer Verlag, 1999.
6. P. Ge and M. Jouaneh, Tracking Control of a Piezoceramic Actuator, *IEEE Transactions on Control System Technology*, 4, pp. 209–216, 1996.
7. R. C. Smith, Inverse Compensation for Hysteresis in Magnetostrictive Transducers, *Mathematical and Computer Modelling*, 33, pp. 285–298, 2001.

8. D. Grant and V. Hayward, Variable Structure Control of Shape Memory Alloy Actuators, *IEEE Contr Syst Mag*, 17(3), pp. 80–88, 1997.
9. J. M. Cruz-Hernandez and V. Hayward, An Approach to Reduction of Hysteresis in Smart Materials, *Proceedings of the 1998 IEEE, International Conference on Robotics & Automation*, pp. 1510–1515, Leuven, Belgium, 1998.
10. G. V. Webb and D. C. Lagoudas, Control of SMA Actuators under Dynamic Environments, *Proc. 6th Ann. Int. Symp. Smart Struct. Mat.*, Newport Beach, USA, 1-5-March 1999, vol. 3667, Newport Beach, USA, 1-5-March 1999, 1999. SPIE.
11. G. Tao and P. V. Kokotovich, *Adaptive Control of Systems with Actuator and Sensor Nonlinearities*, John Wiley and Sons, 1996.
12. P. Ioannou and J. Sun, *Robust Adaptive Control*, Prentice Hall, Englewood Cliffs, NJ, 1996.
13. S. Seelecke and C. Büskens, Optimal Control of Beam Structures by Shape Memory Wires, in Hernandez and C. A. Brebbia, editors, *OPTI 97, Computer Aided Optimum Design of Structures, Rome, Italy, September 8-10, 1997*, pp. 457–466, Rome, Italy, September 8-10, 1997, 1997. Comp. Mech. Press.
14. X. Tan and J. Baras, Optimal Control of Hysteresis in Smart Actuators: A Viscosity Solutions Approach, Springer series LNCS 2289, *Proceedings of the 5th International Workshop on Hybrid Systems: Computation and Control*, pp. 451-464, 2002
15. X. Tan, *Control of Smart Actuators*, Ph. D. dissertation, University of Maryland, College Park, MD, 2002
16. R. C. Smith, A Nonlinear Optimal Control Method for Magnetostrictive Actuators, *Journal of Intelligent Material Systems and Structures*, 9, pp. 468–486, 1998.
17. Stefan Seelecke, *Adaptive Structures with SMA Actuators – Modeling and Simulation (In German)*, Habilitation Thesis, TU Berlin, 1999.
18. N. Papenfuß and S. Seelecke, Simulation and Control of SMA Actuators, *Proc. 6th Ann. Int. Symp. Smart Struct. Mat.*, Newport Beach, USA, 1-5 March, 1999, vol. 3667, pp. 586–595, Newport Beach, USA, 1-5 March, 1999, 1999. SPIE.
19. S. Seelecke and I. Müller, Shape Memory Alloy Actuators in Smart Structures - Modeling and Simulation, *Appl. Mech. Reviews*, 2003, to appear.
20. S. Seelecke, C. Büskens, I. Müller, and J. Sprekels, *Online Optimization of Large Systems: State of the Art*, chapter Real-Time Optimal Control of Shape Memory Alloy Actuators in Smart Structures, Springer Verlag, 2001.
21. R. C. Smith, S. Seelecke, M. J. Dapino and Z. Ounaies, Unified Model for Hysteresis in Ferrous Materials, *SPIE Smart Structures and Materials 2003, Modeling, Signal Processing, and Control*, San Diego, CA, 2003, to appear.
22. R. C. Smith, S. Seelecke and Z. Ounaies, A Free Energy Model for Piezoceramic materials, *SPIE Smart Structures and Materials 2002, Modeling, Signal Processing and Control*, San Diego, CA, 17-22 March 2002, 2002.
23. R. C. Smith and S. Seelecke, An Energy Formulation for Preisach Models, *SPIE Smart Structures and Materials 2002, Modeling, Signal Processing and Control*, San Diego, CA, 17-22 March 2002, 2002.
24. R. C. Smith, S. Seelecke, Z. Ounaies and J. Smith, A Free Energy Model for Hysteresis in Ferroelectric Materials, *Journal of Intelligent Material Systems and Structures*, 2003, submitted.
25. C. Büskens, NUDOCSS – User’s Manual, Universität Münster, 1996.
26. F. Preisach, Über die magnetische Nachwirkung (On the Magnetic Aftereffect), *Zeitschrift für Physik*, 94, pp. 277-302, 1935.
27. W. S. Galinaitis and R. C. Rogers, Compensation for Hysteresis Using Bivariate Preisach Models, *SPIE Smart Structures and Materials 1997, Mathematics and Control in Smart Structures*, San Diego, CA, 1997.
28. P. Ge and M. Jouaneh, Modeling Hysteresis in Piezoceramic Actuators, *Precision Engineering*, 17, pp. 211-221, 1995.
29. W. Chen and C. S. Lynch, A Model for Simulating Polarization Switching and AF-F Phase Changes in Ferroelectric Ceramics, *Journal of Intelligent Material Systems and Structures*, 9, pp. 427-431, 1998.
30. L. Huang and H. F. Tiersten, An Analytic Description of Slow Hysteresis in Polarized Ferroelectric Ceramic Actuators, *Journal of Intelligent Material Systems and Structures*, 9, pp. 417-426, 1998.
31. E. Hairer, G. Wanner, *Solving Ordinary Differential Equations II – Stiff and Differential- Algebraic Problems*, Springer Verlag, 1991.
32. J. Zhong, S. Seelecke, R. C. Smith, Parametrizing Phase Transitions as an Efficient Way to Implement Distributions into Energy-Based Active Material Models, 2003, in preparation.